

PULSED POWER SCIENCES AT SANDIA NATIONAL LABORATORIES – THE NEXT GENERATION*

M. K. Matzen[§]

*Sandia National Laboratories, PO Box 5800
Albuquerque, NM 87185-1190 USA*

Abstract

A combination of theory, simulation, and high-quality experiments has enabled significant progress in many high energy density science applications. While the recent science and engineering of pulsed power has been focused on the refurbishment of Z and developing advanced radiographic capabilities, discovery and innovation in the fundamental architecture of pulsed power systems have also made significant advances. This progress started in 1996 when the Particle Beam Fusion Accelerator (PBFA II), which began operation in 1985, was converted to the Z facility. The Z Refurbishment (ZR) project began six years later, driven by the need for more capacity (the ability to perform more experiments), improved precision (more precise pulse shaping, longer pulses, and reduced jitter), and more capability (higher energy delivered to the load and better diagnostic access). Over the past year, the Z facility was completely dismantled and rebuilt with newly designed components within the same basic 36-module architecture. With the completion of this project in 2007, the pulsed power sciences program at Sandia will work with many collaborators to apply this new capability to many areas of high energy density science, including z-pinch-driven inertial confinement fusion, dynamic materials properties, and radiation hydrodynamics. This paper summarizes recent and planned research on the Z facility, the ZR Project, advances in high-photon-energy radiography, derivative applications of the pulsed power program, and advances in the science of pulsed power that could revolutionize the next-generation facilities.

I. INTRODUCTION

Pulsed power science is a collection of technologies and capabilities that enable us to concentrate electrical energy efficiently in space and time. The combination of theory, simulation, and high-quality experiments has enabled significant progress in many high energy density science (HEDS) applications.

Our objective is to create and understand high energy density environments by conducting highly diagnosed experiments in the following areas: magnetically-driven plasma implosions, magnetically-driven compression waves and flyer plate acceleration, intense and high-average-power particle beam generation, transport, and focusing, high-voltage breakdown phenomenology, and electrostatic discharge physics.

The capabilities that enable these applications are large-scale computations, theory, advanced diagnostics, and the ability to do precision measurements. The large-scale facilities at Sandia National Laboratories available for experiments are the Z pulsed power facility (26 MA, 100 TW, 100 to 300 ns), the Z-Beamlet (2 TW, 1 ns) and Z-Petawatt (500 kJ, 500 fs) laser facilities, and the Radiographic Integrated Test Stand (RITS) facility (120-180 kA, 7-11 MeV, 75 ns).

The Z accelerator, in particular, is a successful experimental platform for HEDS. The first shot on Z was in September 1996. The last shot before shutdown for the ZR Project was in July 2006. Z has operated at 20 MA

and 50 TW on over 1700 shots and results from these experiments have been published in over 160 peer-reviewed journal articles. Descriptions of Z and its capabilities can be found in previous IEEE Pulsed Power Conference proceedings [1-9].

With this combination of capabilities and facilities we have been able to address many HEDS applications such as inertial confinement fusion (ICF) and the physics of materials under high pressure. Spin-off applications include three-dimensional (3D) electromagnetic simulations of large systems that require massively-parallel computer resources, high-brightness flash x-ray radiography, aircraft and mine safety innovations, and engineering of inertial fusion energy systems. We have also developed new pulsed power techniques that enable significant advances in future machine design.

II. HIGH ENERGY DENSITY SCIENCE RESEARCH ON Z

A. Overview

High energy density science experiments are mounted at the center of Z, as shown in Fig. 1. These experiments usually employ cylindrical wire arrays or short-circuit fixed conductors for isentropic compression experiments (ICE). The current from Z provides a $\mathbf{J} \times \mathbf{B}$ force that either implodes a cylindrical wire array producing radiation or provides magnetic pressure for ICE. The

* Sandia is a multi-program laboratory operated by Sandia Corporation, a Lockheed Martin Company, for the United States Department of Energy under Contract DE-AC04-94AL85000.

[§] Email: mkmazze@sandia.gov

energy conversion efficiency is high for a wire-array implosion, with typical x-ray energy $\sim 15\%$ of the stored electrical energy and x-ray power 2 to 4 times the electrical power.

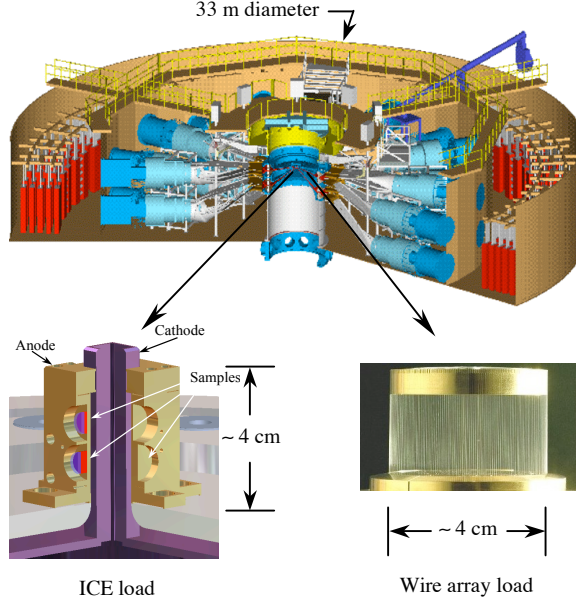


Figure 1. HEDS experiments are mounted at the center of Z.

Diagnosing the imploding plasma is difficult because of the high-power radiation background, but is possible with x-ray backlighting using a bent-crystal imaging (BCI) detector. This technique has allowed diagnosis of the details of plasma implosions as well as diagnosis of the spherical symmetry and minute surface details of radiation-driven imploding targets.

Significant progress has been made in understanding the physics of the z-pinch plasma. The simple model of a thin-shell plasma implosion has been replaced by a more detailed 3D picture with ablated mass from wire arrays, Rayleigh-Taylor (RT) bubble and spike structures, azimuthal currents, and a general web-like structure of the imploding plasma. These effects have been successfully modeled with the 3D ALEGRA code.

Experiments on Z have also validated two-dimensional (2D) radiation-hydrodynamic models of capsule implosions for double-ended hohlraum configurations. This modeling has been extended to a 500-MJ-yield design that has much larger tolerances for radiation pulse tailoring, and ablator surface roughness. These simulations set requirements for the radiation drive and pulsed-power driver for high yield.

By tailoring the time-dependent drive pulse on Z it has been possible to isentropically compress material samples in high-magnetic pressure, short-circuit load configurations. Pressures up to 15 Mbar with pulse lengths up to 300 ns have been achieved.

B. Bent Crystal Imaging Diagnostics

A key diagnostic for many experiments on Z is x-ray backlighting in the 1-10 keV range. X-ray backlighting was used on about 42% of all shots on Z in FY04-FY06. The x-ray backlighting sources are produced using the 2-TW, multi-kJ Z-Beamlet laser (ZBL) [10], which is located in a building to the south of the Z facility. The light from ZBL is transported about 70 m to the Z vacuum chamber, where it is focused to a $\sim 100\text{ }\mu\text{m}$ diameter spot ($\sim 10^{16}\text{ W/cm}^2$) on the surface of a metal-foil target. About 0.1-1 J of x rays has been produced in the 1-10 keV range, depending on the target material chosen, with the conversion efficiency falling off rapidly with increasing photon energy [11].

X-ray backlighting was initially used on Z for point-projection radiography of ICF capsule implosions in a double-ended hohlraum geometry [12,13]. In this geometry, the source, object, and detector are all in a line, so any background and debris produced by the source has a clear line-of-sight to the detector. Because the capsule was located sufficiently far from the z-pinch x-ray sources (each generating $\sim 1\text{ MJ}$ of soft x rays), it was possible through tight collimation to obtain radiographs. For most other applications, however, point-projection radiography was impossible because the z-pinch-produced x-ray background was too high. The spatial resolution obtained on the capsule experiments, 80-100 μm , was limited by the best-available focal spot size of the laser.

A novel backlighting approach using spherically-bent crystals to diffract and focus the imaging x rays can be used to both overcome the background and solve the debris problem while allowing $\sim 10\text{-}\mu\text{m}$ resolution to be obtained over large fields of view [14,15,16]. In this geometry the crystal acts as a spherical mirror, reflecting and focusing only the x rays from the object that satisfy the Bragg diffraction condition onto the detector. The detector sees only the crystal, not the experiment, and hence the background and debris produced by the Z experiment can be blocked. Thus, the x-ray sources produced by ZBL need only exceed the target background at a particular wavelength. Two such systems, one at 1.865 keV and one at 6.151 keV, have been built at Z with demonstrated spatial resolutions of 10-20 μm [17,18,19]. With these imaging systems it has been possible to study even the wire-array z-pinch plasmas themselves. The diagnostic has been used for a variety of z-pinch physics [20,21,22,23,24], ICF capsule [19,25], radiation hydrodynamics [19,26], and dynamic hohlraum [27] experiments.

Example radiographs from ICF double-ended-hohlraum capsule experiments [19] in Fig. 2 illustrate the high spatial resolution possible with the 6.151-keV crystal imaging system. Hundreds of small jets with spatial scales $< 20\text{ }\mu\text{m}$ are visible in the images, which would not have been observable with our point-projection backlighting diagnostic.

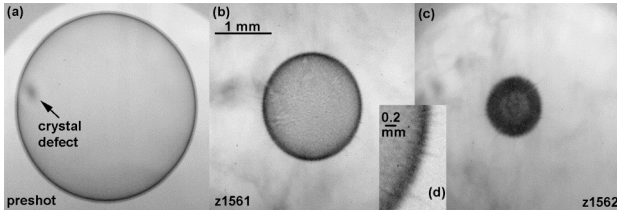


Figure 2. Example 6.151-keV radiographs of a 3.4-mm-diameter plastic ICF capsule inside a double-ended hohlraum taken (a) pre-shot, (b) on Z shot # 1562, and (c) on Z shot # 1561. The capsule was known to have hundreds of large-scale, isolated dome defects on its surface. These apparently produced a myriad of small jets (some $\sim 20 \mu\text{m}$ in diameter on Z shot # 1562 as seen in part (d).) The sharp, dark circle in the pre-shot radiograph is a 1.8 μm glass layer buried partway in the plastic shell.

Although significant quantitative advances have been made in BCI systems, improvements are needed. Each radiograph in Fig. 2 required a separate Z shot. We have been working on a prototype 2-frame, 6.151-keV backlighting system to collect multiple images per shot and on time-gated detectors [19]. The capsule implosions in Fig. 2 occur in ~ 4 ns, so the ~ 1 ns pulse width of ZBL causes significant blurring. Furthermore, because the opacity of the tungsten liner is too high to make quantitative z-pinch physics or capsule measurements near the axis, we are building the Z-Petawatt laser. This laser is nearing completion and will be capable of producing ~ 500 kJ, ~ 500 fs laser pulses. Its short pulse duration will eliminate motional blurring and may provide > 10 -keV photon energies. It is unclear whether crystal-imaging techniques can be extended significantly beyond 10 keV. However, point-projection radiography may be possible above this level since the intensity of the z-pinch-produced x rays falls off significantly above 10 keV.

C. Z-Pinch Physics and 3D Calculations

In recent years, careful analysis of the voltage and current histories for wire-array z-pinch experiments on Z has provided strong evidence that the total current in the wire-array load does not travel to the axis with the leading edge of the imploding plasma. At the beginning of the x-ray power pulse, the mean current radius, as suggested by the load inductance history combined with a thin shell model, is typically found to be 3 to 4 mm away from the axis [28, 29].

It is well established that the imploding wire array plasma extends significantly in radius as a consequence of RT and other instabilities. This left-behind or trailing mass is routinely observed in 2D (r,z) simulations of imploding plasma shells. However, these same 2D simulations fail to reproduce the current at large radius inferred from the inductance unfolds of the experimental

current and voltage histories. One problem inherent in the 2D simulations is the assumption of symmetry in the θ direction. RT instabilities leave mass at larger radius in the characteristic bubble and spike topology, but the axial resistance is extremely high except at the leading edge of the implosion. The extremely high resistance between the spikes greatly inhibits the flow of current at larger radii. Failure to reproduce the experimentally observed radial current distribution leads to unrealistically large and narrow x-ray power pulses in the 2D simulations.

Accurate simulation of a z pinch requires modeling the mass ablation phase, which occupies the first 50-80% of the z-pinch lifetime. During this phase, stationary wire cores cook off material that is swept radially inwards by the $\mathbf{J} \times \mathbf{B}$ force, resulting in a radial redistribution of mass. In fact, axial variations in the mass ablation rate cause the implosion to start before all the mass in the wires has finished ablating, thus providing a mechanism other than the RT instability to explain the trailing mass. Our capabilities with regard to 3D simulations have advanced in recent years with improvements and enhancements to the ALEGRA code. These improvements include modeling the mass ablation phase as a mass inflow boundary condition. By allowing axial variations in the mass ablation rate, we can accurately model the mass distribution at the start of the implosion and the seeding of the RT instabilities.

Just as importantly, in our 3D implosions, we do not assume complete azimuthal correlation of the mass ablation rate, so that the resulting RT growth leads to bubbles that do not extend completely around the axis in θ . As a consequence, a web-like connection of trailing mass is formed and current can travel azimuthally around the imploding bubbles. This radically different topology for 3D versus 2D implosions has two very important consequences. The first is that the RT growth is mitigated as current is shunted around the localized, but high-inductance bubbles and begins to switch to lower inductance, but more resistive, current paths in the web-like trailing mass. The resulting mass distribution shows a much greater degree of correspondence with radiography images than has ever been possible with 2D simulations. The second consequence is that the fading of the current away from the leading edge of the bubble regions and into the trailing mass lowers and broadens the power pulse to the extent that excellent agreement between simulated and experimental power pulses is now possible. These advances in our 3D simulation capability and our understanding of z-pinch dynamics bring us much closer to a predictive capability.

D. Z-Pinch-Driven Double-Ended Hohlraum High Yield Target Design

Double-ended hohlraum experiments on Z in the past several years [30] have validated computational models of hohlraum energetics and radiation symmetry for scaling to larger accelerators. Building on this body of

work and earlier scoping studies [31], recent integrated 2D hohlraum + capsule radiation-hydrodynamics (RHD) simulations have demonstrated adequate hohlraum coupling, time-dependent radiation symmetry control, and the implosion, ignition, and burn of a 500-MJ yield capsule [32]. Figure 3 shows the high-yield double-ended hohlraum target design, centered around a 2.65-mm-radius beryllium ablator capsule containing cryogenic DT fuel. The capsule absorbs 1.2 MJ of x-rays, delivered in three temporally-spaced steps with effective temperatures of 95 eV, 130 eV, and 223 eV that provide nearly-adiabatic fuel compression. The magnitude and timing of the temperature steps can vary by a considerable amount (± 2.8 ns and $\pm 30\%$ in flux for the 95-eV foot) without degrading the yield. Recent 2D multimode RT simulations indicate that the capsule can tolerate an rms ablator surface roughness of 180 nm in modes 12-160, a factor of five above the target fabrication specification of ~ 36 nm for beryllium capsules on the National Ignition Facility [33]. Work is in progress to characterize the capsule tolerance for higher mode numbers and to seek even more robust capsule designs.

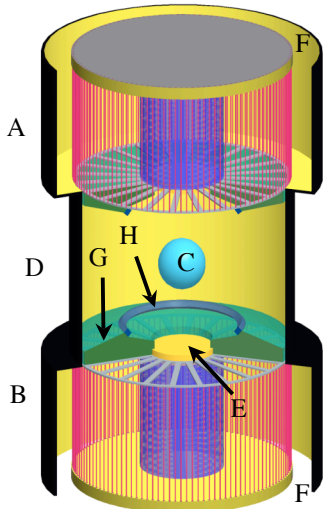


Figure 3. Double-z-pinch hohlraum concept. Top and bottom primary hohlraums (A) and (B) contain notional wire-array z pinches with internal pulse-shaping targets. High yield capsule (C), secondary hohlraum (D) containing the capsule, on-axis permanent shine shield and radial-spoke electrode structures (E), upper and lower electrical power feeds (F), secondary entrance tamping foam (G), P₄ symmetry shield (H)

Hohlraum energetics and radiation symmetry control are studied using 2D LASNEX [34] integrated hohlraum + capsule simulations that currently provide the most complete model of the target. These simulations include the physics of radiation transport, hohlraum wall and symmetry shield RHD, capsule implosion RHD, and capsule ignition and thermonuclear burn. The z-pinch

source is included as a moving cylindrical x-ray source with a prescribed trajectory and prescribed x-ray power history. To determine the z-pinch energy requirements, the x-ray power history is iterated until the calculated incident x-ray flux reproduces the pulse shape used to design the capsule. For the hohlraum system in Fig. 4, the z pinches must produce shaped pulses with a total x-ray output of 18 MJ for the capsule to absorb the required 1.2 MJ. Designing loads to produce the requisite x-ray pulse shape is the subject of ongoing research; currently, multi-shell low-Z loads look the most promising at predicted peak currents of 60-70 MA [35].

For capsule ignition and burn, the relative asymmetry of the x-ray flux to the capsule must be $\sim 1\%$ or less; the double z-pinch hohlraum design achieves time-dependent symmetry control at this level using hohlraum geometry and structures within the hohlraum. Capsule radiation asymmetry is commonly expressed in terms of Legendre modes; the P₂ mode is tuned with secondary hohlraum length [36, 30] and with tamping foams. An unacceptably large inherent P₄ asymmetry led to the new feature of the target design shown in Fig. 3: burn-through shields offset from the capsule that selectively tune certain low-order asymmetry modes (e.g., P₄) and avoid perturbing higher-order modes and without incurring an energy penalty. Using a 4.4°, 200 mg/cc, 450 μm thick P₄ shield as shown in Fig. 3, the inherent -3.3% P₄ during the foot pulse was reduced to -0.3% while maintaining acceptably low values of P₆ and P₈ asymmetry. Negative P₄ values of several percent have been measured under foot-like conditions on Z [30], and the use of shields to tune P₄ will be validated in future experiments. Properly chosen tamping foams and P₄ burn-through shields result in simulated compressed DT fuel configurations with a calculated yield of 470 MJ. Capsule yields of 400-500 MJ have been obtained in 2D simulations for a range of tamping foams, and P₄ burn-through shield sizes, with or without magnetic tamping of the primary hohlraum walls, and with or without early run-in radiation emitted by the z pinches. Preliminary accelerator design studies [37,38] show that machines with stored energies of approximately 400 MJ may be compatible with this hohlraum target design; future advances in compact x-ray source development could significantly lower the stored energy requirement. Target design is underway to determine the hohlraum coupling and symmetry control requirements for higher hohlraum efficiency.

E. ICE and Flyer Plate Experiments

In Z experiments for material dynamics studies at high stresses, independent triggering of the pulse-forming modules is used to provide ~ 20 MA, ~ 300 ns rise-time, shaped current pulses. The resulting order of several megagauss magnetic fields produce quasi-isentropic compression of the short-circuit load conductors over the discharge time of the machine [39,40] with magnetic pressures approaching 400 GPa (4 Mbar).

Planar stress waves are generated in centimeter-sized material samples. Typically, four anode panels are arranged about a central stainless steel or tungsten cathode post, forming a symmetric anode-cathode gap. 2D magneto hydrodynamic (MHD) calculations show that magnetic field uniformity of $\sim 0.5\%$ can be obtained over the central horizontal region of the anode plate [41]. Up to five samples can be stacked vertically on a panel. The magnetic pressure induces a hydrodynamic stress wave that propagates into the anode material that can be used in ICE. A recent example of the ICE technique is found in references [42, 43], where the high-pressure compression response of aluminum is inferred by measuring its stress up to 250 GPa.

Since ramp loading produces continuous loading curves, the measured stress-strain response is sensitive to small changes in material response. Thus the technique is well suited for the study of first-order phase transitions. An elegant example is the recent work of Dolan, et al. on water [44]. In these experiments thin ($\sim 20 \mu\text{m}$) samples between sapphire and cubic zirconia windows were ramp loaded to peak stresses of ~ 14 GPa. Measured stress profiles at the rear water/window interface are shown in Fig. 4. A pronounced, transient drop in stress was observed in all water samples at ~ 7 GPa. Based on the known equilibrium properties of water, isentropic compression should drive the sample into the stable phase of solid ice VII at ~ 2 GPa. Prior experiments using silica windows do show evidence of partial freezing over 10–100 ns timescales when compressed to over 2 GPa [45]. In sharp contrast, the latest experiments exhibit extremely rapid (within a few ns), complete freezing at a pressure of 7 GPa. These results provide compelling evidence that water reaches a hyper-cooled state at 7 GPa and that freezing nucleates homogeneously [44].

A successful spin-off of the ICE technique has been developed to magnetically accelerate flyer plates to ultra-high velocities [46]. The technique uses the magnetic field produced in the insulating gap to impulsively load the anode, providing momentum and launching it as an effective flyer plate to high velocity. The highest velocity achieved to date is 34 km/s. Each anode panel becomes a flyer plate by machining the entire current-carrying portion of the aluminum anode panel to a prescribed material thickness of $\sim 800\text{--}900 \mu\text{m}$. To retain rigidity and to allow the panels to be assembled together, this flyer frame is attached to a panel back. The panel back also allows mounting of the targets at a prescribed distance from the flyer plate, typically $\sim 3\text{--}4$ mm, and mounting of optical probes used to diagnose the targets. Each panel back can hold several separate targets, allowing multiple and simultaneous shock wave experiments during a single firing of Z.

The magnetically accelerated flyer plate technique has been used to help resolve a recent controversy in the compressibility of hydrogen and its isotopes at high pressure. Flyer plate experiments were performed to

obtain Hugoniot data for liquid deuterium using an impedance matching method [47, 48] up to ~ 120 GPa, as given in ref [49]. These results have been compared to experimental results using light-gas guns [50], a laser drive [51, 52] and a multi-stage explosive device [53, 54]. Except for the laser Hugoniot experiments, the results agree with data from the other experimental approaches and with the theories for deuterium [55,56], with the exception of the Ross model [57]. This good agreement gives confidence that the shock compression response of deuterium up to ~ 120 GPa is well established.

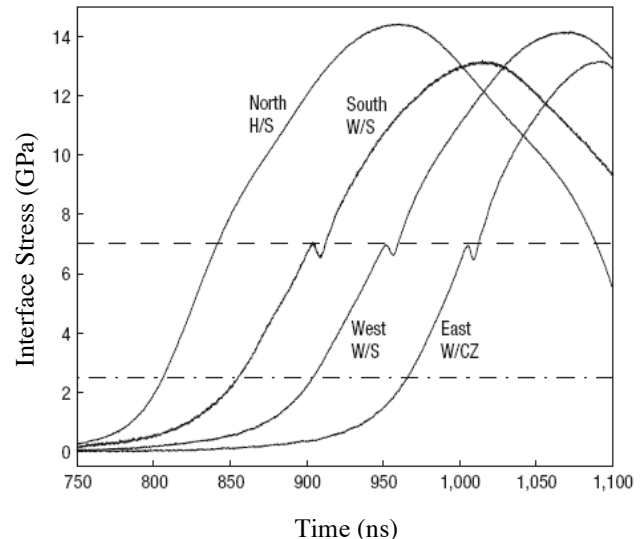


Figure 4. Interface stress histories for isentropically compressed water and hexane. The abbreviations indicate the sample (water, W, or hexane, H) and window (sapphire, S, or cubic zirconia, CZ) materials. Hexane was used as a control, as no phase transition is expected in this pressure range. The dashed line indicates the prompt transition threshold near 7 GPa, whereas the dash-dot line indicates the pressure at which liquid water becomes metastable. The plots have been time shifted by 50 ns for visual clarity; actual compressions are nearly coincident.

A significant benefit of the ultra-high velocity flyer plate technique is the ability to perform complex loading experiments at extreme pressures. Experiments can be performed with composite flyer plates, fabricated with layers of material with different shock impedance, capable of imparting finite duration shock loading followed by well defined pressure release. By measuring the shock and release wave profiles through multiple thicknesses of the sample, the wave speed of the material in the shocked state can be inferred by a wave overtaking method [58]. The wave speed is sensitive to the state of the material, with a solid exhibiting a noticeably higher wave speed than a liquid. By measuring the wave speed over a span of Hugoniot pressures, the shock pressure at which melt begins can be determined. Experiments of

this type have recently been performed on beryllium and diamond to examine the strength and melt properties along the principal Hugoniot in support of the National Ignition Campaign. The results of these experiments, which will be the subject of future publications, have provided new insight into the melt properties and have significantly improved our understanding of these materials in the high energy density regime.

III. SELECTED APPLICATIONS OF PULSED POWER TECHNOLOGY

A. Overview

Detailed modeling of complicated pulsed-power components for the ZR Project and other pulsed-power applications has led to improved capabilities in electromagnetic and plasma physics codes.

We are also developing a high-energy flash x-ray source for defense science applications by applying electron-beam diode technology using inductive voltage adders. Significant progress has been achieved, with the measured radiation quality about a factor of five from the ultimate goal.

The development of electromagnetics (EM) and pulsed power sciences for the nuclear weapons complex has led to spin-off benefits in other arenas. Recent examples include the development of the Pulsed Arrested Spark Discharge wiring diagnostic, and EM analysis that determined a probable cause of the Sago mine disaster in January 2006.

There has also been a modest effort in the pulsed sciences program to develop a roadmap for application of inertial fusion energy to economical power production. This effort presumes that single-shot, high-yield fusion with pulsed-power drivers is achievable and seeks to address questions relevant to transforming this technology to high repetition-rate, low-cost, reliable operation. A power-plant architecture has been developed, and a number of critical design issues have been addressed and resolved.

B. Advances in 3D EM Computational Capabilities

Sandia has developed a number of high physical fidelity, general purpose, EM and plasma physics codes for a wide array of applications. A primary application is computational analysis of large pulsed power machines. We have used these codes to predict the performance of large sections of the refurbished Z to circumvent some construction and testing of expensive prototypes. The EIGER™ frequency-domain Maxwell's equations code has been used to determine the optimal number of water switches, and the EMPHASIS™ time-domain, finite-element Maxwell's equations code has been used to calculate the transient EM fields in detail for the water convolute and to derive accurate lumped parameters for the system circuit model (Fig. 5). Finally, we have used

our QUICKSILVER time-domain, EM particle-in-cell code to model the magnetically insulated vacuum powerflow and the transient EM fields in the laser-triggered gas switches.

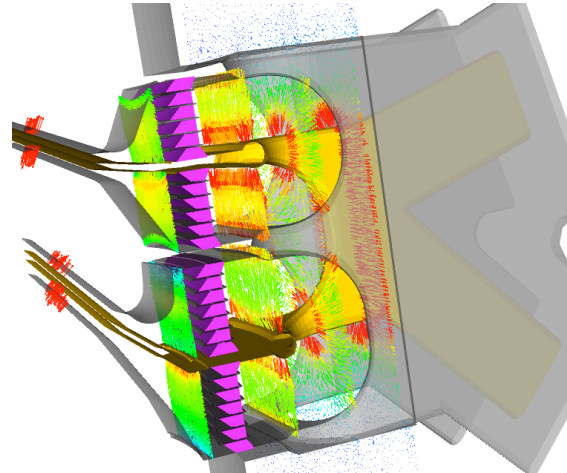


Figure 5. Calculated electric field vectors at an instant in time in the water convolute section of ZR.

These codes can be executed on platforms from desktop computers to massively-parallel systems with the latter enabling simulations of exceptional size and geometric fidelity. We are continuing to develop these codes for improved predictions of the performance of pulsed power systems.

C. Progress in Radiography

The Radiographic Integrated Test Stand [59] is an Inductive Voltage Adder (IVA) accelerator developed at Sandia National Laboratories for driving high brightness flash x-ray radiographic sources. The x-ray sources are high-power electron beam diodes. In its present configuration, RITS-6, six induction cells are driven by 8-ohm parallel water-dielectric pulse forming lines (PFLs). The individual induction cells are joined in series by a vacuum, coaxial magnetically insulated transmission line (MITL) that delivers power from the cells to the diode region. The geometry of the accelerator and diode region is shown in Fig. 6. RITS-6 is capable of producing 7-11 MeV, 120-180 kA, 75-ns-pulse-length electron beams. These beams are focused onto high-Z x-ray converter targets with power densities in excess of 10 TW/cm².

The figure of merit (FOM) of such sources is usually quantified by the radiation intensity and defined as

$$FOM = \frac{\text{dose}}{\text{spot}^2} \text{ (rad/mm}^2\text{)}, \quad (1)$$

where the dose (rads) is defined at 1 meter from the source and the spot size is defined in terms of an equivalent, fully-filled Gaussian distribution.

A long-term objective is to maximize the FOM. Over the next few years, experiments will be conducted on RITS-6 to enhance and optimize the x-ray intensity of the next generation sources, with the goal of achieving a greater than five-fold increase in x-ray intensity compared to present-day pulsed-power-driven sources. Presently we are achieving record FOMs for this type of system with sources that produce > 300 rads at one meter and spot sizes ~ 2.7 mm in 50-ns-long radiation pulses corresponding to a FOM > 40 [60]. The long-term goal is to demonstrate sources with a FOM of ~ 200 .

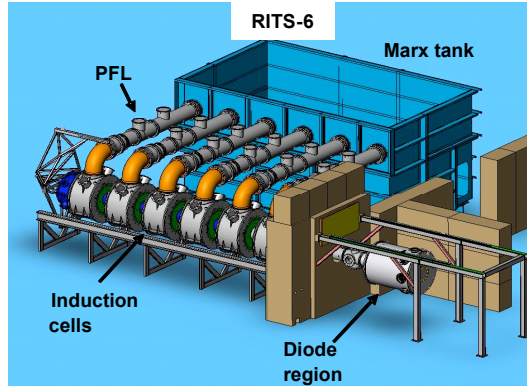


Figure 6. Illustration of the RITS-6 accelerator and diode region.

D. Spin-off Applications of Pulsed Power Technology

Two significant applications of pulsed power technology are the Pulsed Arrested Spark Discharge (PASD) diagnostic technique, and the simulation of the Sago mine disaster, which led to new standards for the mining industry.

PASD, a short-pulse high-voltage wiring insulation diagnostic, is effective in detecting and locating a variety of insulation defects in complex wiring geometries [61,62] (Fig. 7). PASD is highly immune to line impedance variations, an important characteristic for applications in aircraft wiring systems, and has been shown to be nondestructive to electrical insulation materials. The Sandia patented concept was implemented as a versatile portable diagnostic called ArcSafe® by

Astronics Advanced Electronics Systems. ArcSafe® was commercialized in early 2007. Sandia's work on PASD received an *R&D 100* award by *R&D Magazine* and was recognized with an *Interagency Partnership Award* by the Federal Laboratory Commission in competition with over 250 federal laboratories. PASD shows great promise as an effective diagnostic to find difficult-to-locate insulation defects including breached insulation, chaffing, and physically small insulation cracks in a wide array of applications.

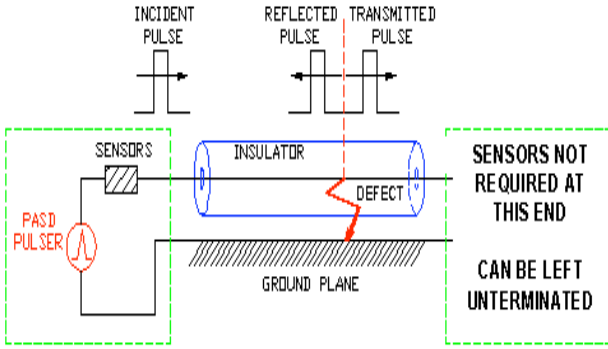


Figure 7. Diagram of the PASD wiring diagnostic as applied to wiring harnesses in aircraft.

Through the use of analysis and field measurement techniques developed to secure nuclear weapons facilities against lightning, a team from Sandia's Pulsed Power Sciences Center postulated and demonstrated the first-ever coupling of indirect lightning energy (propagated without the presence of electrical conductors) into an abandoned and sealed shaft at the Sago mine. The sealed shaft, which had filled with an explosive mixture of methane gas, exploded during a lightning storm, leading to the deaths of twelve miners. Ten similar events have occurred since 1993 without a clear indication of cause. Electromagnetic field measurements with highly sensitive instrumentation were used to generate transfer functions relating surface lightning events to coupled voltage into an abandoned pump cable in the sealed shaft [63]. The simulations showed that the induced voltage in the cable could have been as high as 25 kV, with pulse duration of nearly 200 μ sec, which certainly could have led to arcing at an unterminated end. This modeling, analysis, and field measurements led to a revision of mine safety procedures for abandoned mine shafts by the Mine Safety and Health Administration [64].

E. Z-Pinch Inertial Fusion Energy

Z-pinch inertial fusion energy (Z-IFE) study complements and extends Sandia's z-pinch fusion program to a *repetitive*, high-yield, power plant scenario that could be used for the production of electricity, transmutation of nuclear waste, and hydrogen production. The long-range goal of Z-IFE is to produce an economically-attractive power plant using high-yield z-

pinch-driven targets ($\sim 3\text{GJ}$) with low rep-rate per chamber ($\sim 0.1\text{ Hz}$).

The present concept for a Z-IFE power plant uses a repetitive pulsed power driver (the LTD, or linear transformer driver), a recyclable transmission line (RTL), a dynamic hohlraum z-pinch-driven target, and a thick liquid-wall chamber. The RTL connects the pulsed power driver directly to the z-pinch-driven target, and is made from frozen coolant or a material that can be easily separable from the coolant (such as low activation ferritic steel). The fusion explosion destroys the RTL, but the RTL materials are recycled, and a new RTL is inserted on each shot. The approach to a 1000 MWe Z-IFE power plant is evolving. An artist's concept of a z-pinch fusion chamber for such a plant is shown in Fig. 8.

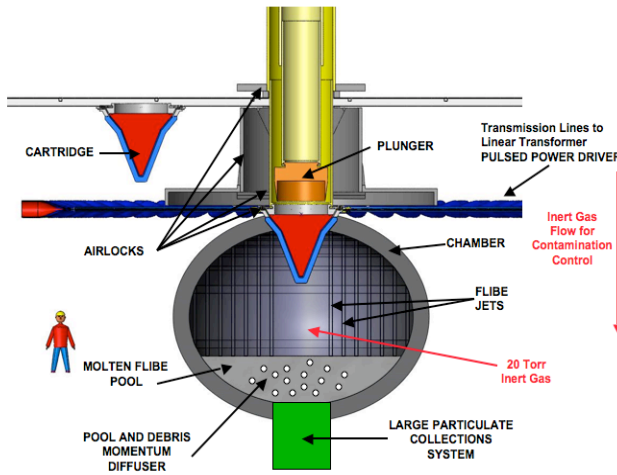


Fig. 8. Artist's concept of the fusion reaction chamber in a Z-IFE power plant.

A development path for Z-IFE has been created that complements and leverages the pulsed power ICF program. Research has been focused on (1) RTLs, (2) repetitive pulsed power drivers, (3) shock mitigation (because of the high-yield targets), (4) planning for a proof-of-principle full RTL cycle demonstration (with a 1 MA, 1 MV, 100 ns, 0.1 Hz driver), (5) IFE target studies for multi-GJ yield targets, and (6) z-pinch IFE power plant engineering and technology development. Much of the research has been focused on two critical components of this concept, the RTLs and the pulsed power driver [65].

Key physics issues for RTLs involving the power flow at the high linear current densities that occur near the target (up to 5 MA/cm) have been investigated. These issues include surface heating, melting, ablation, plasma formation, electron flow, magnetic insulation, conductivity changes, magnetic field diffusion changes, possible ion flow, and RTL mass motion. These issues have been studied theoretically, computationally, and experimentally. Present results indicate that RTLs will

work at 5 MA/cm or higher, with anode-cathode gaps as small as 2 mm. An RTL misalignment sensitivity study has been performed using a 3D circuit model. The load current variations are small for significant RTL misalignments. The structural issues for RTLs have also been addressed.

Repetitive operation of a 0.5-MA, 90-kV, 100-ns LTD cavity with gas purging between shots and automated operation has been demonstrated at the SNL Z-IFE LTD laboratory with rep-rates up to 10.3 seconds between shots. (The 10.3-second rep rate is essentially the 10-second goal for Z-IFE). A single LTD switch was fired repetitively every 12 seconds for 36,000 shots with no failures. Five 1.0-MA, 100-kV, 100-ns LTD cavities have been combined into a voltage adder configuration with a test load to study the system operation. The combination of multiple LTD coaxial lines into a tri-plate transmission line has been examined. The 3D QUICKSILVER code was used to study the electron flow losses near the magnetic nulls that occur where coax LTD lines are added together. Circuit model codes have been used to model the complete power flow circuit with an inductive isolator cavity.

LTD architectures for Z-IFE and high yield facilities have also been developed and these are discussed in Section V. Present results from power flow studies validate the LTD/RTL concept for single-shot ICF high yield and for repetitive-shot IFE.

IV. Z REFURBISHMENT PROJECT

Z has enabled critical experiments that addressed many Stockpile Stewardship Program (SSP) and HEDS needs. The energetic (1.6 MJ), intense ($> 200\text{ TW}$) Z provides x rays for radiation effects testing, radiation transport and hydrodynamics experiments, and ICF to perform equation of state (EOS) experiments by directly utilizing the high magnetic fields associated with the short-pulse, high-current-density, large-current flow. The magnetic pressures reached in ICE and high velocity flyer plate configurations are unique for performing dynamic material property experiments.

Z's roots go back to 1985 when the facility was constructed as PBFA II, designed to produce high voltages (10 - 30 MV) in a single-gap diode to accelerate and focus ions on millimeter-sized fuel pellets to study controlled fusion. As a result of breakthroughs achieved on the 2-MV, 10-MA Saturn accelerator with z-pinch technology, PBFA II was modified in 1996 to provide high current rather than a high voltage in order to run a six-month set of scaling experiments for z pinches, after which the machine was scheduled to return to light-ion research. Only the center vacuum stack and water line attachments were modified for this short campaign. Because of the ongoing success of z pinches, the machine was never converted back for light-ion research, and was renamed Z in July 1997.

Because operational efficiency of Z was limited by the age of hardware and to specifically design the pulsed-power drive system for z-pinch applications, we initiated the ZR Project, which was formally initiated with Critical Decision 0 (CD-0) in February 2002. The plan was to refurbish Z with modern, conventional technology and systems optimized for z pinches as well as design for durability. The Project goals were to increase utilization by providing capacity to perform more shots, improve overall precision and pulse shape variability for better reproducibility and data quality, and increase the delivered current to allow additional performance capability. Improvements have been accomplished within the existing building and exterior tank structure, and will enhance Sandia's pulsed power capabilities in several key areas well into the next decade.

The facility improvements include:

- New Marx generator capacitors, doubling the energy storage capability within the same capacitor volume,
- A combined energy diverter/prefire protection system between the Marx generators and intermediate storage capacitors,
- Individual lasers for the laser triggered gas switches, providing the main pulse shaping capability (lasers were installed in January 2003),
- Intermediate storage capacitors electrically optimized for a balance between the short-pulse mode (100 ns) for wire-array experiments, and the long-pulse mode ($\sim > 300$ ns) for material property experiments, with high electrical reliability in either mode,
- A less expensive laser-triggered gas switch design, located in oil to reduce the likelihood of electrical breakdown,
- A single-stage, electrically-optimized pulse forming line, replacing the three stage hardware from the original PBFA II system,
- Stainless steel construction for durability, and
- A greatly enhanced diagnostic infrastructure to provide versatility, adaptability, and more diagnostics capacity.

Following a two-year single-line design/test phase and a two-year production design and fabrication phase, Z was taken off line on July 26, 2006 for refurbishment. During this past year, significant modifications were made to the tank structure, a new oil/water separation wall was constructed, and the majority of the pulsed power components and subsystems were assembled and installed. Following completion of the hardware installation and electrical/mechanical utility construction, subsystem testing will take place leading to full system demonstration shots at reduced voltage, forecast for September 2007. Project completion (CD-4) is anticipated in September 2007 with the transition to routine experimental operations occurring over the subsequent six months.

V. NEXT GENERATION PULSED-POWER TECHNOLOGY

A. Overview

Significant advances in pulsed-power techniques have been developed in the past few years. Of most importance is the LTD technology, jointly developed with the Russians and the French. This technology has been applied to a proposed design for a 1-PW-class z-pinch driver, and promises improvements in simplicity and reliability. Similar techniques are being applied to developing lower current, tailored pulse drivers for intermediate-pressure dynamic materials measurements.

B. Linear Transformer Drivers

The development of LTDs [66-92] is a major advance in prime-power generation for pulsed-power accelerators since the invention of the Marx generator in 1924. Conventional Marxes work well and are a mature technology, but necessitate subsequent pulse compression to achieve the short pulses ($<< 1$ μ s) required to drive z pinches and other loads of interest to the HEDS community. LTDs are less mature, but can directly produce much shorter pulses than conventional Marxes. Consequently, an LTD-driven pulsed-power accelerator promises to be, at a given load current and pulse width, more efficient and reliable. Seminal work by Kovalchuk et al. [66,69,76,81], Bastrikov et al. [67,79], Kim et al. [68,72,74,75,78,80,83,91], McDaniel and Spielman [70], Savage [71], Mazarakis et al. [73,77,88,92], Rose et al. [82,90], Vizir et al. [84], Leckbee et al. [85,86,89], and Rogowski et al. [87] have led to impressive advances in LTD technology. As a result, LTDs are becoming an attractive alternative to conventional Marx generators.

Both Marxes and LTDs charge capacitors in parallel and discharge them in series. However, an LTD module does this as an *inductive voltage adder*, in which each of the adder's cavities is driven by capacitors and switches that are *contained within the cavity*.

An LTD "module" is a linear array of stacked annular LTD "stages" in a voltage-adding configuration. An LTD stage is also referred to as a "cavity." Proposed LTD modules for future accelerators consist of as many as 70 LTD cavities stacked in series [37,77,88]. Fig. 9 illustrates how a 3-cavity LTD module would function. When the switches in each cavity close at time τ_{cav} later than the switches in the previous cavity, then an entire n -cavity LTD module can be modeled as a single *RLC* circuit [37,73,87,88].

The peak power generated by such a time-synchronized LTD module is optimized when the output impedance of the module Z_{opt} is given by the following expression [37]:

$$Z_{\text{opt}} = 1.10 \sqrt{\frac{L_{\text{mod}}}{C_{\text{mod}}}} + 0.80R_{\text{mod}}, \quad (2)$$

where L_{mod} is the total series inductance of the module, C_{mod} is the series capacitance, and R_{mod} is the series

resistance. When $R_{\text{mod}} \ll \sqrt{L_{\text{mod}}/C_{\text{mod}}}$, the peak output power P_{LTD} of such an impedance-matched module is given by [37]:

$$P_{\text{LTD}} = 0.33 \frac{n_{\text{cav}}^2 V_{\text{cav}}^2}{Z_{\text{opt}}} , \quad (3)$$

where n_{cav} is the number of cavities in the module, and V_{cav} is the initial total charge voltage of a single LTD cavity. This expression is consistent with 1D circuit models and 2D EM simulations.

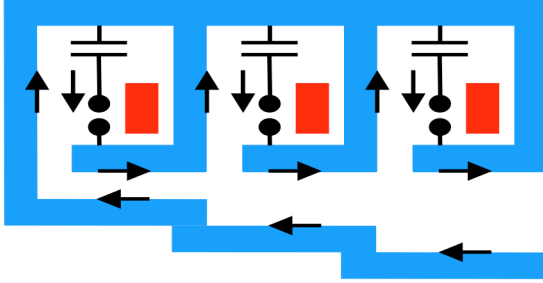


Figure 9. (a) Idealized representation of a 3-cavity LTD module. Each cavity can contain a large number of capacitors and switches; these are represented here by a single capacitor and a single switch. The red rectangles represent magnetic cores. The arrows represent the path of *most* of the current flow, after all the switches have closed. We neglect here the small fraction of the current that flows around the inductive cores.

Proposed future LTD-driven accelerators would require as many as 210 LTD modules, each of which would consist of as many as 60-70 LTD cavities [37,77,88]. References [37,77,88] assume that each cavity, in turn, would include 40 switches and 80 capacitors. Given how many components such a machine would require, it is natural to ask how reliable it would be. We find that such a machine would be extremely reliable since (1) the switches and capacitors in the LTD cavities are operated at relatively low voltages (~ 200 kV), and (2) in general, as the current and voltage of such components in an accelerator are decreased, *the total accelerator reliability increases faster than the number of components* [94].

In fact, we estimate that an LTD-based machine may be as much as *three orders of magnitude more reliable* than a comparable Marx-based driver [37]. This estimate is based on measurements by Kim and colleagues at the High Current Electronics Institute [93] and Mazarakis and colleagues at Sandia National Laboratories [94]. Kim et al. find that a single LTD switch driven by two capacitors has a lifetime in excess of 40,000 shots [93]. Mazarakis et al. find that a prototype 0.5-MA LTD cavity that contains 20 switches and 40 capacitors has a lifetime in excess of 13,000 shots [94]. These measurements have also demonstrated that an LTD cavity can achieve a timing jitter of 2 ns and voltage and current reproducibilities of 0.3% [94].

C. Architecture of Petawatt-Class Z-Pinch Accelerators

Recent calculations suggest that accelerators with electrical powers in excess of 1000 TW would be required to drive z-pinch implosions that radiate in excess of 1000 TW of x-ray power [38]. Such radiated powers would enable large-diameter ICF-capsule-implosion experiments [38,95-112] and other HEDS experiments [113-119] to be conducted over heretofore-inaccessible parameter regimes. Consequently, it is of interest to consider how a petawatt-class z-pinch accelerator might be designed.

A number of architectures have been proposed for future pulsed-power z-pinch drivers [68,77,88,111,120-128]. In this article, we briefly review a new architecture [37] that was motivated by, and builds upon, previous designs. The architecture can be driven by various types of electrical-pulse generators, such as Marx generators. We consider herein a version of the architecture that is driven by LTD modules. The LTD-driven architecture is described in more detail in Ref. [37] and is illustrated in Fig. 10. As suggested by this figure, the architecture includes an LTD section, a water section, and a vacuum section. The LTD section encircles the water section, which in turn encircles the vacuum section. The three sections have cylindrical geometries, and are concentric.

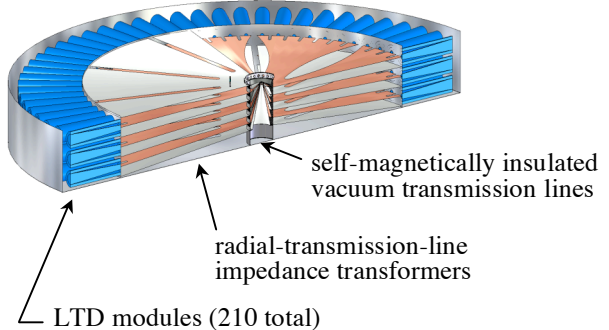


Figure 10. 3D model of a 1000-TW LTD-based z-pinch accelerator. The model is approximately to scale. The diameter of the outer-tank wall is 104 m [37,88]. The model shows a person standing on the uppermost water-section electrode, near the central vacuum section.

The LTD-based architecture includes the following: (1) several stacked levels of LTD modules, (2) a coaxial water-insulated matched-impedance transmission line within each LTD, (3) several stacked levels of monolithic triplate radial-transmission-line impedance transformers, that are water insulated and have exponential impedance profiles, (4) a multilevel insulator stack, (5) a multilevel MITL system, and (6) a vacuum post-hole convolute.

The new architecture has been applied to the design of a 1000-TW pulsed power accelerator [37]. The accelerator has 210 modules, each containing 60 LTD cavities. The modules store 182 MJ and generate a peak electrical power of 1200 TW, of which 1080 TW arrives

at the insulator stack. The accelerator delivers an effective peak current of 68 MA to a z pinch that implodes in 95 ns and 75 MA to a pinch that implodes in 120 ns.

D. Compact Pulser for ICE Research

The success of z-pinch driven shock physics and EOS experiments on Z demonstrated the viability of high-current drivers to produce extraordinary data sets. Building on this concept, Sandia is developing a small (5-mm diameter) platform capable of producing 4.5 MA current into target loads optimized for EOS experiments. The drive current can be shaped to accommodate various density materials through the use of a multimodular design with approximately 230 modules and 60 programmable trigger points. Current shape requirements are driven by the desire to eliminate shock waves, allowing for greater lengths of time for which 1D measurements of the material response behavior can be made. The modular design of this system is shown in Fig 11. Each module will produce approximately 20 kA in a package that can be unplugged for replacement or servicing. Target output parameters include the production of 250 kBar in 20 x 50 mm wide sample panels. Trigger timing for the driver modules will be determined through the use of a genetic algorithm to determine the optimum current shape to produce the desired pressure wave profile for a given material [129].

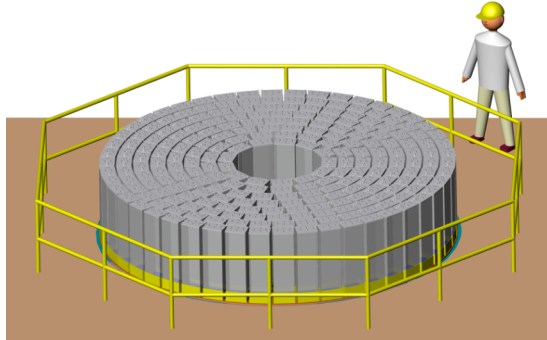


Figure 11. 4.5 MA driver with programmable current shaping capabilities. Each module contains two low-inductance capacitors and a 200-kV air-insulated switch.

The trigger system is a major cost element in this multimodular approach. Advanced switch trigger techniques are being pursued, including the use of low-cost photoconductive semiconductor units located in each module and the use of low-energy (microjoule) laser triggering. Full system design and subsystem testing should be completed in 2008.

VI. SUMMARY

A combination of theory, simulations, and high quality experiments has enabled significant progress in high energy density science and related applications. This progress has been enabled by the development of new pulsed-power platforms and the related theory and computations that have supported and guided experiments. New applications of this have important national benefits in many areas.

The Z accelerator has made important contributions to ICF research, benefiting the national efforts in this endeavor. Dynamic material property studies have reached a new level of precision and capability on Z. Radiation hydrodynamics and radiation effects work have benefited from the x-ray radiation produced by the high-temperature plasmas generated in the load regions of Z.

Electromagnetics and pulsed power are being applied to new areas, such as aircraft and mine safety. Compact machines are being developed to enable inexpensive and more precise dynamic materials research.

The combined refurbished Z, Z-Beamlet, and Z-Petawatt will provide an exciting experimental platform for future work. These upgrades promise a higher number of shots, more precise and flexible data, and greater capability in producing higher currents and higher plasma temperatures.

The LTD technology looks promising for many pulsed power applications and is now being applied to concepts of new machine architectures that promise high reliability, simplicity, and new capabilities.

VII. ACKNOWLEDGEMENTS

Thanks to the following individuals for providing specific input for this publication: D. D. Bloomquist, M. E. Cuneo, M. P. Desjarlais, M. C. Herrmann, M. L. Kiefer, M. D. Knudson, M. G. Mazarakis, T. A. Mehlhorn, B. V. Oliver, C. L. Olson, J. L. Porter, L. X. Schneider, D. B. Sinars, W. A. Stygar, R. A. Vesey, and E. A. Weinbrecht. Special thanks to K. W. Struve and M. A. Sweeney for work to assemble and edit the final manuscript.

VIII. REFERENCES

- [1] R. B. Spielman *et al.*, in *Proceedings of the 11th IEEE International Pulsed Power Conference*, edited by G. Cooperstein and I. Vitkovitsky (IEEE, Piscataway, NJ, 1997), p. 709.
- [2] P. Corcoran, *et al.*, *ibid.*, p. 466.
- [3] R. J. Garcia, *et al.*, *ibid.*, p. 1614.
- [4] H. C. Ives, *et al.*, *ibid.*, p. 1602.
- [5] R. W. Shoup, *et al.*, *ibid.*, p. 1608.
- [6] D. L. Smith, *et al.*, *ibid.*, p. 168.
- [7] K. W. Struve, *et al.*, *ibid.*, p. 162.
- [8] W. A. Stygar, *et al.*, *ibid.*, p. 591.
- [9] W. A. Stygar, *et al.*, *ibid.*, p. 1258.
- [10] P. Rambo *et al.*, *Appl. Optics* **44**, 2421 (2005).
- [11] L. E. Ruggles, J.L. Porter, P.K. Rambo, W.W. Simpson, M.F. Vargas, G.R. Bennett, and I.C. Smith, *Rev. Sci. Instrum.* **74**, 2206 (2003).
- [12] G. R. Bennett, *et al.*, *Phys. Rev. Lett.* **89**, 245002 (2002).
- [13] R. A. Vesey, *et al.*, *Phys. Rev. Lett.* **90**, 035005 (2003).
- [14] S. A. Pikuz, *et al.*, *Rev. Sci. Instrum.* **68**, 740 (1997).
- [15] Y. Aglitskiy, *et al.*, *Rev. Sci. Instrum.* **70**, 530 (1999).
- [16] J. A. Koch, *et al.*, *Rev. Sci. Instrum.* **70**, 525 (1999).
- [17] D. B. Sinars, G.R. Bennett, D.F. Wenger, M.E. Cuneo, and J.L. Porter, *Appl. Optics* **42**, 4059 (2003).
- [18] D. B. Sinars, G.R. Bennett, D.F. Wenger, *et al.*, *Rev. Sci. Instrum.* **75**, 3672-3677 (2004).
- [19] G. R. Bennett, D.B. Sinars, D. F. Wenger, *et al.*, *Rev. Sci. Instrum.* **77**, 10E322 (2006).
- [20] D. B. Sinars, M.E. Cuneo, E. P. Yu, *et al.*, *Phys. Rev. Lett.* **93**, 145002 (2004).
- [21] D. B. Sinars, M.E. Cuneo, B. Jones, *et al.*, *Phys. Plasmas* **12**, 056303 (2005).
- [22] M. E. Cuneo, D.B. Sinars, D. E. Bliss, *et al.*, *Phys. Rev. Lett.* **94**, 225003 (2005).
- [23] D. B. Sinars, M.E. Cuneo, E. P. Yu, *et al.*, *Phys. Plasmas* **13**, 042704 (2006).
- [24] D. B. Sinars, M. E. Cuneo, S. V. Lebedev, *et al.*, "Radiation energetics of inertial confinement fusion relevant wire-array z pinches," submitted to *Phys. Rev. Lett.* (2007).
- [25] G. R. Bennett, *et al.*, "First observations of fill-tube induced mass perturbations on x-ray-driven, ignition-scale, inertial-confinement fusion capsule shells, and the implications for ignition experiments," submitted to *Phys. Rev. Lett.* (2007).
- [26] R. R. Peterson, D. L. Peterson, R. G. Watt, G. Idzorek, T. Tierney, and M. Lopez, *Phys. Plasmas* **13**, 056901 (2006).
- [27] G. A. Chandler, D. B. Sinars, K. Peterson, *et al.*, *Bull. Amer. Phys. Soc.* **50**, BP1 132 (2005).
- [28] E. M. Waisman, M. E. Cuneo, W. A. Stygar, R. L. Lemke, K. W. Struve, and T. C. Wagoner, *Phys. Plasmas* **11**, 2009 (2004).
- [29] M. E. Cuneo, E. M. Waisman, S. V. Lebedev, *et al.*, *Phys. Rev. E* **71**, 046406 (2005).
- [30] M. E. Cuneo, R. A. Vesey, G. R. Bennett, *et al.*, *Plasma Phys. Control. Fusion* **48**, R1 (2006) and references therein.
- [31] J. H. Hammer, M. Tabak, S. C. Wilks, J. D. Lindl, D. S. Bailey, P. W. Rambo, A. Toor, G. B. Zimmerman, and J. L. Porter, *Phys. Plasmas* **6**, 2129 (1999).
- [32] R. A. Vesey, M. C. Herrmann, R. W. Lemke, M. P. Desjarlais, M. E. Cuneo, W. A. Stygar, G. R. Bennett, R. B. Campbell, P. J. Christenson, T. A. Mehlhorn, J. L. Porter, and S. A. Slutz, *Phys. Plasmas* **14**, 056302 (2007).
- [33] S. W. Haan (private communication, 2006); A. Nikroo, K. C. Chen, M. L. Hoppe, *et al.*, *Phys. Plasmas* **13**, 056302 (2006).
- [34] G. B. Zimmerman and W. L. Kruer, *Comm. Plas. Phys. Contr. Fusion* **2**, 51 (1975).
- [35] R. W. Lemke, R. A. Vesey, M. E. Cuneo, M. P. Desjarlais, and T. A. Mehlhorn, "Z-pinch requirements for achieving high yield fusion via a z-pinch driven, double ended hohlraum concept," to appear in *Proceedings of Megagauss XI*, 2007.
- [36] R. A. Vesey, M. E. Cuneo, J. L. Porter, *et al.*, *Phys. Plasmas* **10**, 1854 (2003).
- [37] W. A. Stygar, M. E. Cuneo, D. I. Headley, H. C. Ives, R. J. Leeper, M. G. Mazarakis, C. L. Olson, J. L. Porter, T. C. Wagoner, and J. R. Woodworth, *Phys. Rev. ST Accel. Beams* **10**, 030401 (2007).
- [38] W. A. Stygar, M. E. Cuneo, R. A. Vesey, H. C. Ives, *et al.*, *Phys. Rev. E* **72**, 026404 (2005).
- [39] J. R. Asay, in *Shock Compression of Condensed Matter – 1999*, edited by M.D. Furnish, L. C. Chhabildas, and R. S. Hixson (AIP, New York, 1999) p. 261.
- [40] R. W. Lemke, M. D. Knudson, A. C. Robinson, T. A. Haill, K. W. Struve, J. R. Asay, and T. A. Mehlhorn, *Phys. Plasmas* **10**, 1867 (2003).
- [41] D. B. Reisman, A. Toor, R. C. Cauble, C. A. Hall, J. R. Asay, M. D. Knudson, and M. D. Furnish, *J. Appl. Phys.* **89**, 1625 (2001).
- [42] J-P Davis, *J. Appl. Phys.* **99**, 103512 (2006).
- [43] D. B. Hayes and C. A. Hall, in *Shock Compression of Condensed Matter – 2001*, edited by M.D. Furnish, N. Thadhani, and Y. Horie (AIP, New York, 2001) p. 1177.
- [44] D. A. Dolan, M. D. Knudson, C. A. Hall, and C. Deeney, *Nature Physics* **3**, 339 (2007).
- [45] D. A. Dolan and Y. M. Gupta, *J. Chem. Phys.* **121**, 9050 (2004); *J. Chem. Phys.* **123**, 64702 (2005).
- [46] R. W. Lemke, M. D. Knudson, D. E. Bliss, K. Cochrane, J-P Davis, A. A. Giunta, H. C. Harjes, and S. A. Slutz, *J. Appl. Phys.* **98**, 073530 (2005).

[47] M. D. Knudson, D. L. Hanson, J. E. Bailey, C. A. Hall, J. R. Asay, and W. W. Anderson, Phys. Rev. Lett. **87**, 225501 (2001).

[48] M. D. Knudson, D. L. Hanson, J. E. Bailey, C. A. Hall, J. R. Asay, and C. Deeney, Phys. Rev. B **69**, 144209 (2004).

[49] M. D. Knudson, J. R. Asay, and C. Deeney, J. Appl. Phys. **97**, 073514 (2005).

[50] W. J. Nellis, A. C. Mitchell, M. van Thiel, G. J. Devine, and R. J. Trainor, J. Chem. Phys. **79**, 1480 (1983).

[51] L. B. Da Silva, *et al.*, Phys. Rev. Lett. **78**, 483 (1997).

[52] G. W. Collins, *et al.*, Science **281**, 1178 (1998).

[53] S. I. Belov, *et al.*, Sov. Phys. JETP Lett. **76**, 433 (2002).

[54] G. V. Boriskov, *et al.*, Dokl. Phys. **48**, 553 (2003).

[55] G. I. Kerley, Sandia National Laboratories Report SAND2003-3613, 2003.

[56] M. P. Desjarlais, Phys. Rev. B **68**, 064204 (2003).

[57] M. Ross, Phys. Rev. B **58**, 669 (1998).

[58] R. G. McQueen, J. W. Hopson, and J. N. Fritz, Rev. Sci. Instrum. **53**, 245 (1982).

[59] I. D. Smith, *et al.*, Proc. 12th IEEE Intl. Pulsed Power Conf., Monterey, CA 1999, p. 403.

[60] B. V. Oliver and J. E. Maenchen “Advanced X-ray Radiography on the RITS-6 Accelerator”, to appear in the Proc. 1st Euro-Asian Pulsed Power Conf., EAPPC, Sept. 18-22, 2006.

[61] R. K. Howard, S. F. Glover, G. E. Pena, L. X. Schneider, M. B. Higgins, “Final Report on Development of Pulse Arrested Spark Discharge (PASD) for Aging Aircraft Wiring Applications”, Sandia National Laboratories Report, SAND2005-2638, September 2006.

[62] S. F. Glover, M. B. Higgins, G. E. Pena, L. X. Schneider, “Assessment of the Non-Destructive Nature of PASD on Wire Insulation Integrity”, Sandia National Laboratories Report, SAND2003-3430, September 2003.

[63] M. B. Higgins, M. E. Morris, “Measurement and Modeling of Transfer Functions for Lightning Coupling into the Sago Mine”, Sandia National Laboratories Report, SAND2006-7976, April 2007.

[64] R. A. Gates, *et al.*, “Report of Investigation: Fatal Underground Coal Mine Explosion, January 2, 2006, Sago Mine, Wolf Run Mining Company”, ID No. 46-08791, Department of Labor, Mine Safety and Health Administration, May 9, 2007.

[65] C. L. Olson, *et al.*, “Recyclable Transmission Line (RTL) and Linear Transformer Driver (LTD) Development for Z-Pinch Inertial Fusion Energy (Z-IFE) and High Yield,” Sandia National Laboratories Report, SAND2007-0059, January 2007.

[66] B. M. Kovalchuk, V. A. Vizir, A. A. Kim, E. V. Kumpjak, S. V. Loginov, A. N. Bastrikov, V. V. Chervjakov, N. V. Tsou, Ph. Monjaux, and D. Huet, Sov. Izv. Vuzov. Phys. **40**, 25 (1997).

[67] A. N. Bastrikov, A. A. Kim, B. M. Kovalchuk, E. V. Kumpjak, *et al.*, in *Proceedings of the 11th IEEE International Pulsed Power Conference*, edited by G. Cooperstein and I. Vitkovitsky (IEEE, Piscataway, NJ, 1997), p. 489.

[68] A. A. Kim, B. M. Kovalchuk, V. V. Kremnev, E. V. Kumpjak, *et al.*, in *Proceedings of the 11th IEEE International Pulsed Power Conference*, edited by G. Cooperstein and I. Vitkovitsky (IEEE, Piscataway, NJ, 1997), p. 862.

[69] B. M. Kovalchuk, in *Proceedings of the 11th IEEE International Pulsed Power Conference*, edited by G. Cooperstein and I. Vitkovitsky (IEEE, Piscataway, NJ, 1997), p. 59.

[70] D. H. McDaniel and R. B. Spielman (unpublished).

[71] M. E. Savage (unpublished).

[72] A. A. Kim, B. M. Kovalchuk, E. V. Kumpjak, and N. V. Zoi, in *Proceedings of the 12th IEEE International Pulsed Power Conference*, edited by C. Stallings and H. Kirbie (IEEE, Piscataway, NJ, 1999), p. 955.

[73] M. G. Mazarakis and R. B. Spielman, in *Proceedings of the 12th IEEE International Pulsed Power Conference*, edited by C. Stallings and H. Kirbie (IEEE, Piscataway, NJ, 1999), p. 412.

[74] A. A. Kim and B. M. Kovalchuk, in *Proceedings of the 12th Symposium on High Current Electronics* (Institute of High Current Electronics, Tomsk, Russia, 2000), p. 263.

[75] A. A. Kim, B. M. Kovalchuk, A. N. Bastrikov, V. G. Durakov, S. N. Volkov, and V. A. Sinebryukhov, in *Proceedings of the 13th IEEE International Pulsed Power Conference*, edited by R. Reinovsky and M. Newton (IEEE, Piscataway, NJ, 2001), p. 1491.

[76] B. M. Kovalchuk, A. A. Kim, E. V. Kumpjak, N. V. Zoi, and V. B. Zorin, in *Proceedings of the 13th IEEE International Pulsed Power Conference*, edited by R. Reinovsky and M. Newton (IEEE, Piscataway, NJ, 2001), p. 1488.

[77] M. G. Mazarakis, R. B. Spielman, K. W. Struve, and F. W. Long, in *Proceedings of the 13th IEEE International Pulsed Power Conference*, edited by R. Reinovsky and M. Newton (IEEE, Piscataway, NJ, 2001), p. 587.

[78] A. A. Kim, A. N. Bastrikov, S. N. Volkov, V. G. Durakov, B. M. Kovalchuk, and V. A. Sinebryukhov, *Proceedings of the 14th International Conference on High-Power Particle Beams* (2002), p. 81.

[79] A. N. Bastrikov, V. A. Vizir, S. N. Volkov, V. G. Durakov *et al.*, Lasers Part. Beams **21**, 295 (2003).

[80] A. A. Kim, A. N. Bastrikov, S. N. Volkov, V. G. Durakov, B. M. Kovalchuk, and V. A. Sinebryukhov, in *Proceedings of the 14th IEEE International Pulsed Power Conference*, edited by

M. Giesselmann and A. Neuber (IEEE, Piscataway, NJ, 2003), p. 853.

[81] B. M. Kovalchuk, A. A. Kim, E. V. Kumpjak, and N. V. Tsou, in *Proceedings of the 14th IEEE International Pulsed Power Conference*, edited by M. Giesselmann and A. Neuber (IEEE, Piscataway, NJ, 2003), p. 1455.

[82] D. V. Rose, D. R. Welch, B. V. Oliver, J. E. Maenchen, D. C. Rovang, D. L. Johnson, A. A. Kim, and B. M. Kovalchuk, in *Proceedings of the 14th IEEE International Pulsed Power Conference*, edited by M. Giesselmann and A. Neuber (IEEE, Piscataway, NJ, 2003), p. 845.

[83] A. A. Kim, A. N. Bastrakov, S. N. Volkov, V. G. Durakov, B. N. Kovalchuk, and V. A. Synebrukhov, *Proceedings of the 13th International Symposium on High Current Electronics* (Institute of High Current Electronics, Tomsk, Russia, 2004), p. 141.

[84] V. A. Vizir, A. D. Maksimenko, V. I. Manylov, and G. V. Smorudov, *Proceedings of the 13th International Symposium on High Current Electronics* (Institute of High Current Electronics, Tomsk, Russia, 2004), p. 198.

[85] J. J. Leckbee, J. E. Maenchen, S. Portillo, S. R. Cordova, I. Molina, D. L. Johnson, D. V. Rose, A. A. Kim, R. Chavez, and D. R. Ziska, to be published in the Proceedings of the 15th IEEE International Pulsed Power Conference (IEEE, Piscataway, NJ, 2007).

[86] J. J. Leckbee, J. E. Maenchen, S. Portillo, S. R. Cordova, I. Molina, D. L. Johnson, A. A. Kim, R. Chavez, and D. Ziska, to be published in the Proceedings of the 15th IEEE International Pulsed Power Conference (IEEE, Piscataway, NJ, 2007).

[87] S. T. Rogowski, W. E. Fowler, M. G. Mazarakis, C. L. Olson, D. H. McDaniel, K. W. Struve, and R. A. Sharpe, to be published in the Proceedings of the 15th IEEE International Pulsed Power Conference (IEEE, Piscataway, NJ, 2007).

[88] M. G. Mazarakis, W. E. Fowler, F. W. Long, D. H. McDaniel, C. L. Olson, S. T. Rogowski, R. A. Sharpe, and K. W. Struve, to be published in the Proceedings of the 15th IEEE International Pulsed Power Conference (IEEE, Piscataway, NJ, 2005).

[89] J. J. Leckbee, J. E. Maenchen, D. L. Johnson, S. Portillo, D. M. Van De Valde, D. V. Rose, and B. V. Oliver, *IEEE Trans. Plasma Sci.* **34**, 1888 (2006).

[90] D. V. Rose, D. R. Welch, B. V. Oliver, J. J. Leckbee, J. E. Maenchen, D. L. Johnson, A. A. Kim, B. M. Kovalchuk, and V. A. Sinebryukhov, *IEEE Trans. Plasma Sci.* **34**, 1879 (2006).

[91] A. A. Kim, V. G. Durakov, S. N. Volkov, A. N. Bastrakov *et al.*, *Proceedings of the 14th International Symposium on High Current Electronics* (Institute of High Current Electronics, Tomsk, Russia, 2006), p. 297.

[92] M. G. Mazarakis, W. E. Fowler, D. H. McDaniel, A. A. Kim, C. L. Olson, S. T. Rogowski, R. A. Sharpe, and K. W. Struve, *Proceedings of the 14th International Symposium on High Current Electronics* (Institute of High Current Electronics, Tomsk, Russia, 2006), p. 226.

[93] A. A. Kim, *et al.* (unpublished).

[94] M. G. Mazarakis, W. E. Fowler, and R. T. Rogowski, and R. A. Sharpe (unpublished).

[95] J. H. Hammer, M. Tabak, S. C. Wilks, J. D. Lindl, D. S. Bailey, P. W. Rambo, A. Toor, G. B. Zimmerman, and J. L. Porter, *Phys. Plasmas* **6**, 2129 (1999).

[96] R. J. Leeper, T. E. Alberts, J. R. Asay, P. M. Baca, *et al.*, *Nuclear Fusion* **39**, 1283 (1999).

[97] M. E. Cuneo, R. A. Vesey, J. H. Hammer, J. L. Porter, Jr., L. E. Ruggles, and W. W. Simpson, *Laser Part. Beams* **19**, 481 (2001).

[98] M. E. Cuneo, R. A. Vesey, J. L. Porter, G. A. Chandler, *et al.*, *Phys. Plasmas* **8**, 2257 (2001).

[99] M. E. Cuneo, R. A. Vesey, J. L. Porter, G. R. Bennett, *et al.*, *Phys. Rev. Lett.* **88**, 215004 (2002).

[100] G. R. Bennett, M. E. Cuneo, R. A. Vesey, J. L. Porter, *et al.*, *Phys. Rev. Lett.* **89**, 245002 (2002).

[101] D. L. Hanson, R. A. Vesey, M. E. Cuneo, J. L. Porter, *et al.*, *Phys. Plasmas* **9**, 2173 (2002).

[102] R. A. Vesey, M. E. Cuneo, G. R. Bennett, J. L. Porter, R. G. Adams, R. A. Aragon, P. K. Rambo, L. E. Ruggles, W. W. Simpson, and I. C. Smith, *Phys. Rev. Lett.* **90**, 035005 (2003).

[103] G. R. Bennett, R. A. Vesey, M. E. Cuneo, J. L. Porter, *et al.*, *Phys. Plasmas* **10**, 3717 (2003).

[104] R. A. Vesey, M. E. Cuneo, J. L. Porter, R. G. Adams, R. A. Aragon, P. K. Rambo, L. E. Ruggles, W. W. Simpson, I. C. Smith, and G. R. Bennett, *Phys. Plasmas* **10**, 1854 (2003).

[105] R. A. Vesey, M. E. Cuneo, G. R. Bennett, D. Hanson, J. L. Porter, L. E. Ruggles, W. W. Simpson, T. A. Mehlhorn, and S. E. Wunsch, *Bull. Am. Phys. Soc.* **48**, 207 (2003).

[106] R. E. Olson, G. A. Chandler, M. S. Derzon, D. E. Hebron, *et al.*, *Fusion Technol.* **35**, 260 (1999).

[107] T. W. L. Sanford, R. E. Olson, R. L. Bowers, G. A. Chandler, *et al.*, *Phys. Rev. Lett.* **83**, 5511 (1999).

[108] J. E. Bailey, G. A. Chandler, S. A. Slutz, I. Golovkin, *et al.*, *Phys. Rev. Lett.* **92**, 085002 (2004).

[109] C. L. Ruiz, G. W. Cooper, S. A. Slutz, J. E. Bailey, *et al.*, *Phys. Rev. Lett.* **93**, 015001 (2004).

[110] R. E. Olson, *Fusion Sci. Tech.* **47**, 1147 (2005).

[111] C. L. Olson, “Z-pinch inertial fusion energy”, in *Landolt-Boernstein Handbook on Energy Technologies*, editor-in-chief: W. Martienssen, volume VIII/3 of *Fusion Technologies*, edited by K. Heinloth, (Springer-Verlag, Berlin-Heidelberg, 2005).

[112] R. A. Vesey, M. C. Herrmann, R. W. Lemke, M. P. Desjarlais, *et al.*, accepted for publication in *Phys. Plasmas* (2007).

[113] M. D. Rosen, *Phys. Plasmas* **3**, 1803 (1996).

[114] M. K. Matzen, *Phys. Plasmas* **4**, 1519 (1997).

[115] M. A. Liberman, J. S. DeGroot, A. Toor, and R. B. Spielman, *Physics of High-Density Z-Pinch Plasmas* (Springer, New York, 1999).

[116] D. D. Ryutov, M. S. Derzon, and M. K. Matzen, *Rev. Mod. Phys.* **72**, 16 (2000).

[117] J. E. Bailey, G. A. Chandler, D. Cohen, M. E. Cuneo, *et al.*, *Phys. Plasmas* **9**, 2186 (2002).

[118] J. M. Foster, B. H. Wilde, P. A. Rosen, T. S. Perry, M. Fell, M. J. Edwards, B. F. Lasinski, R. E. Turner, and M. L. Gittings, *Phys. Plasmas* **9**, 2251 (2002).

[119] T. W. L. Sanford, T. J. Nash, R. E. Olson, D. E. Bliss, *et al.*, *Plasma Phys. Control. Fusion* **46**, B423 (2004).

[120] J. J. Ramirez, in *Proceedings of the 10th IEEE International Pulsed Power Conference*, edited by W. Baker and G. Cooperstein (IEEE, Piscataway, NJ, 1995), p. 91.

[121] T. H. Martin (unpublished).

[122] K. W. Struve and D. H. McDaniel, *Proceedings of the 12th International Conference on High-Power Particle Beams (Beams '98)*, edited by M. Markovits and J. Shiloh (IEEE, Haifa, Israel, 1998), p. 334.

[123] P. Sincerny, M. Danforth, C. Gilbert, A. R. Miller, T. Naff, W. Rix, C. Stallings, E. Waisman, and L. Schlitt, *Proceedings of the 12th IEEE International Pulsed Power Conference*, edited by C. Stallings and H. Kirbie (IEEE, Piscataway, NJ, 1999), p. 479.

[124] K. W. Struve, J. P. Corley, D. L. Johnson, D. H. McDaniel, R. B. Spielman, and W. A. Stygar, in *Proceedings of the 12th IEEE International Pulsed Power Conference*, edited by C. Stallings and H. Kirbie (IEEE, Piscataway, NJ, 1999), p. 493.

[125] P. Corcoran, I. Smith, P. Spence, A. R. Miller, E. Waisman, C. Gilbert, W. Rix, P. Sincerny, L. Schlitt, and D. Bell, in *Proceedings of the 13th IEEE International Pulsed Power Conference*, edited by R. Reinovsky and M. Newton (IEEE, Piscataway, NJ, 2001), p. 577.

[126] D. H. McDaniel, M. G. Mazarakis, D. E. Bliss, J. M. Elizondo, *et al.*, in *Dense Z Pinches: the Proceedings of the 5th International Conference on Dense Z Pinches*, edited by J. Davis, C. Deeney, and N. Pereira, AIP Conf. Proc. **651** (AIP, Melville, NY, 2002), p. 23.

[127] P. Spence, P. Corcoran, J. Douglas, T. Tucker *et al.*, in *Dense Z Pinches: the Proceedings of the 5th International Conference on Dense Z Pinches*, edited by J. Davis, C. Deeney, and N. Pereira, AIP Conf. Proc. **651** (AIP, Melville, NY, 2002), p. 43.

[128] I. D. Smith, *Phys. Rev. ST Accel. Beams* **7**, 064801 (2004).

[129] S. F. Glover, K. W. Reed, F. E. White, "Genetic Optimization for Pulsed Power System Configuration," *IEEE International Pulsed Power and Plasma Science Conference*, Albuquerque, NM, 2007.